

III. Environmental Requirements

PROJECT ENGINEERING DIVISION

A. Engineering Models of the Venus Atmosphere, R. A. Schiffer

Additional scientific measurements and theoretical studies are required before a clear understanding of the structure of the Venus atmosphere can be evolved. In the meantime, Venus atmosphere engineering models reflecting the best current knowledge are still needed for space vehicle design and mission planning. Accordingly, an interim set of standard models¹ based on the latest scientific data has been prepared; however, they should not be considered as new scientific models of the Venus atmosphere.

Although the combination of parameters into "worst-case" models is a recognized function of the specific mission design, it is not certain that all extremes have been met by the models presented. However, these models may be regarded as a state-of-the-art approximation that envelop current uncertainties of the Venus atmospheric parameters with an estimated confidence of at least 95%.

¹Schiffer, R. A., "Engineering Models of the Venus Atmosphere Based on an Interpretation of Recent Space Vehicle Observations of Venus," paper to be presented at the AIAA 7th Aerospace Sciences Meeting, Jan. 1969.

In preparing these models, particular attention was given to assessing the atmospheric environmental interactions that influence the integrity and performance of a planetary vehicle and its major subsystems. These atmospheric interactions are both aerodynamic and thermal and are directly related to the structure, composition, and dynamics of the atmosphere. Table 1 summarizes these interactions with the principal space vehicle subsystems, and identifies the atmospheric parameters involved in each case. The vertical distribution of mass density is regarded as the most critical parameter for design functions that involve aerodynamic interactions. However, adequate definition of other quantities as chemical composition and temperature structure is also important because they are implicit in the calculation of density and appear as parameters in thermal calculations. In addition, the viscosity, specific heat, and speed of sound influence the vehicle aerothermodynamic analyses, while atmospheric winds primarily affect terminal descent entry dynamics. Finally, the atmospheric aerosol content and opacity constrain the design of landed solar power systems and influence the performance of communications equipment.

Six atmospheric engineering models of the Venus atmosphere are proposed for space vehicle design based

Table 1. Orbiter, entry, and lander vehicle atmospheric environmental interactions

Space vehicle subsystem	Pressure profile	Temperature profile	Density profile	Specific heat	Viscosity	Speed of sound	Gas composition	Winds	Opacity and aerosols
Structural			✓	✓	✓	✓		✓	
Retardation			✓	✓	✓	✓	✓	✓	
Propulsion	✓	✓	✓	✓	✓	✓	✓	✓	✓
Heat shield			✓	✓	✓	✓	✓		
Guidance	✓	✓	✓			✓		✓	
Attitude control	✓	✓	✓			✓		✓	
Communications	✓		✓				✓		✓
Power supply	✓	✓	✓				✓	✓	✓
Electronics	✓	✓	✓				✓		✓
Mechanical devices	✓	✓	✓					✓	✓
Thermal control	✓	✓	✓	✓	✓		✓	✓	✓
Systems analyses	✓	✓	✓	✓	✓	✓	✓	✓	✓

on the theoretical Venus thermal model of McElroy (Ref. 1) and data from the recent *Mariner V* and *Venera 4* space probes (Refs. 2 and 3). The models, which are based on the constraints summarized in Table 2, describe profiles for temperature, density, pressure, speed of sound, molecular mass, density scale height, number density, mean free path, and viscosity. These parameters were calculated by numerical integration of the hydrostatic equation with the aid of thermodynamic relationships (Footnote 1). Figures 1 and 2 illustrate the profiles of temperature and density for each model. Models MV-1 and -2 correspond to minimum solar activity, MV-3 and -4 to moderate solar activity, and MV-5 and -6 to maximum solar activity. Models MV-1, -3, and -5 are high-density models characterized by high pressure and low molecular weight. Models MV-2, -4, and -6 are low-density models characterized by low pressure and high molecular weight. Uncertainties in the knowledge of the dynamics of the Venus atmosphere preclude the specification of a realistic wind model. In addition, no acceptable model describing the aerosol content and opacity is currently available.

The models can be described in the form of probability density functions. However, limitations in the number of data points and in the identification of the experimental errors of currently available scientific data do not permit statistical treatment of the uncertainty ranges for such key parameters as surface pressure, temperature, and composition.

A superposition of the *Mariner V* and *Venera 4* temperature and pressure data interpretations (Figs. 3 and 4)

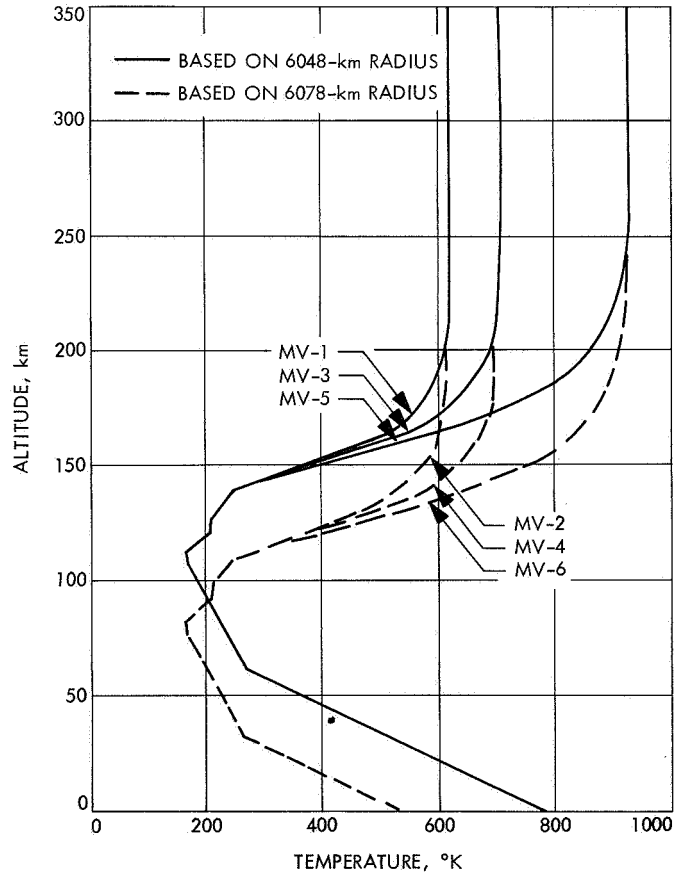


Fig. 1. Temperature vs altitude in Venus atmosphere

results in profiles that agree remarkably well, provided the planetary surface at the *Venera 4* final data transmission point is located at a radius of approximately 6078 km.

Table 2. Parameters for Venus atmosphere models MV-1 through MV-6

Parameter	Minimum solar activity		Mean solar activity		Maximum solar activity	
	MV-1 (high density)	MV-2 (low density)	MV-3 (high density)	MV-4 (low density)	MV-5 (high density)	MV-6 (low density)
Surface pressure, atm	167	16.4	167	16.4	167	16.4
Composition, mole fraction:						
CO ₂	0.81	0.9998	0.81	0.9998	0.81	0.9998
N ₂	0.0998	0	0.0998	0	0.0998	0
CO	0.045	0	0.045	0	0.045	0
O	0.045	0	0.045	0	0.045	0
He	0.0001	0.0001	0.0001	0.0001	0.0001	0.0001
H ₂	0.0001	0.0001	0.0001	0.0001	0.0001	0.0001
Molecular mass, gm/mole	40.42	44	40.42	44	40.42	44
Surface temperature, °K	770	534	770	534	770	534
Exosphere temperature, °K	625	625	710	710	931	931
Planetary radius, km	6048	6078	6048	6078	6048	6078
Surface gravity, cm/s ²	888.1	879.4	888.1	879.4	888.1	879.4
Density at turbopause, g/cm ³	3.6×10^{-11}	3.6×10^{-11}	3.6×10^{-11}	3.6×10^{-11}	3.6×10^{-11}	3.6×10^{-11}

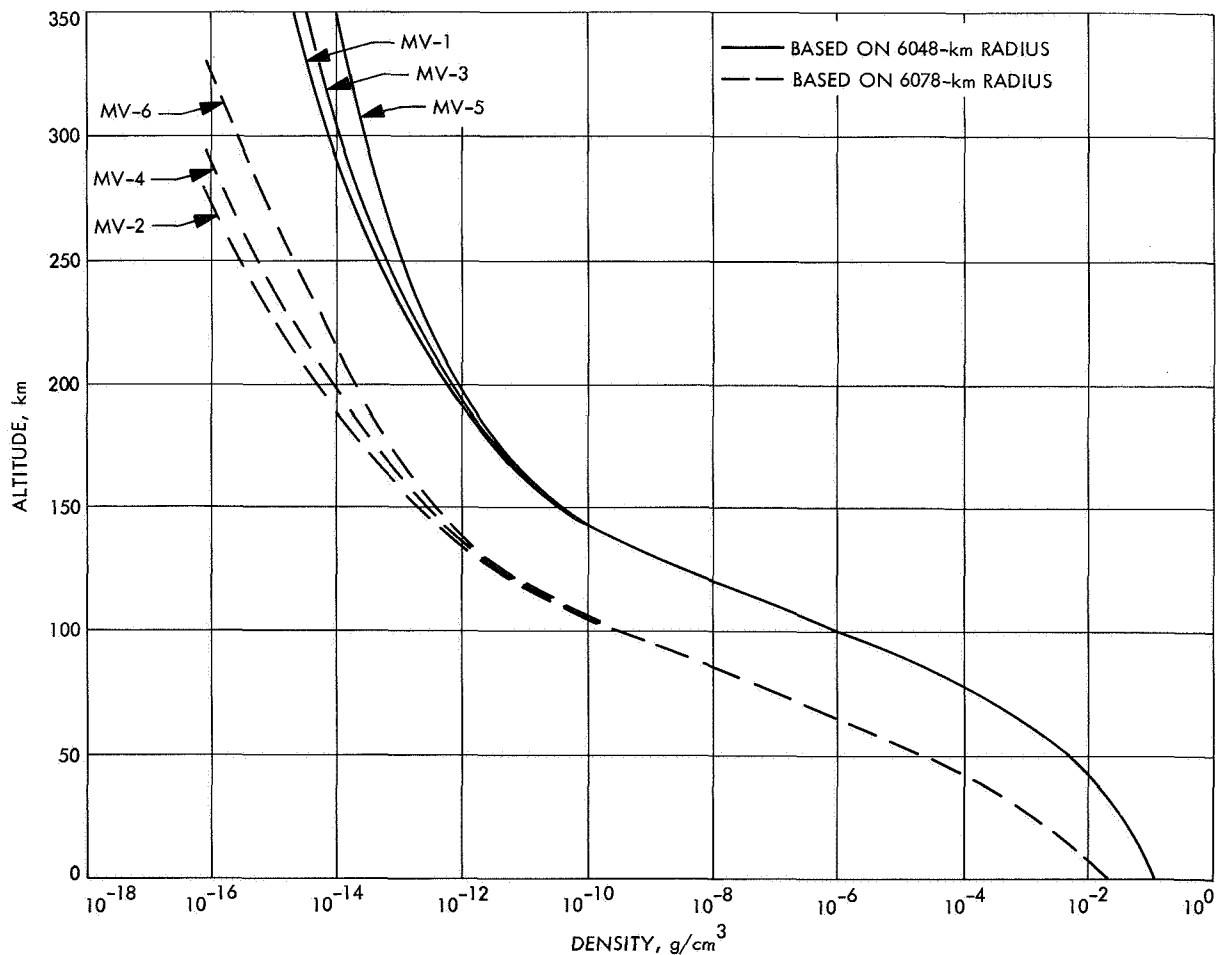


Fig. 2. Density vs altitude in Venus atmosphere

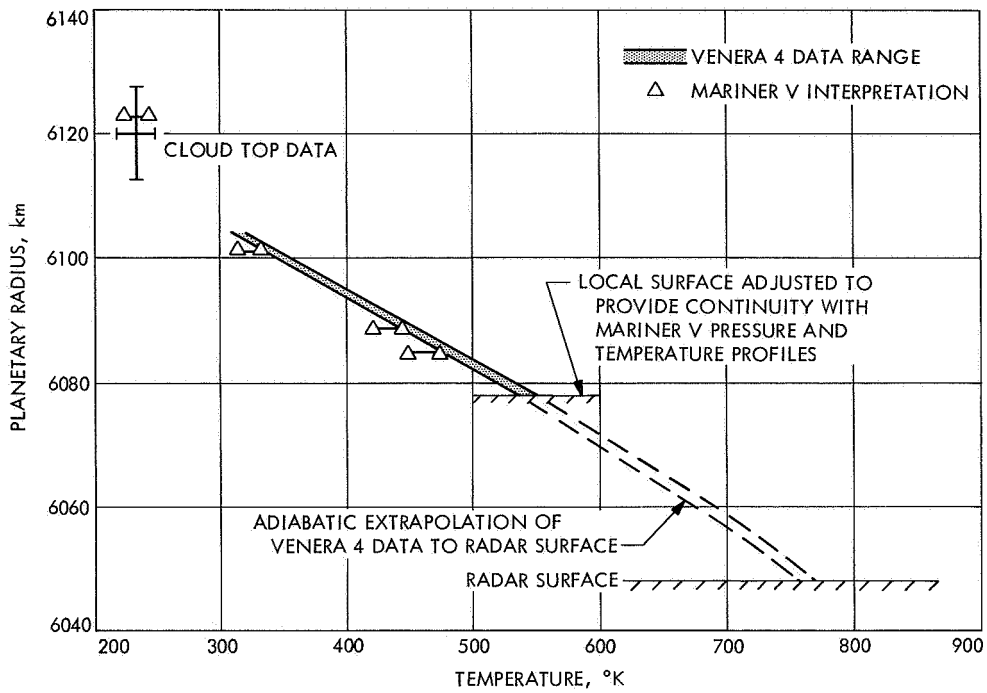


Fig. 3. Venus atmosphere temperature data

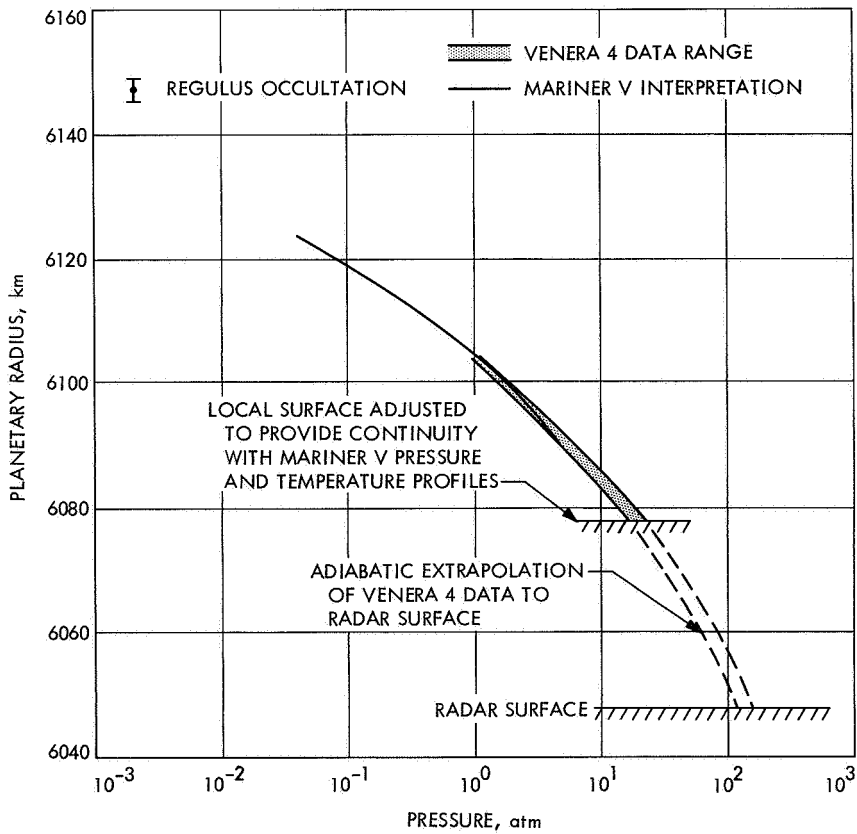


Fig. 4. Venus atmosphere pressure data

However, recent Massachusetts Institute of Technology radar studies of Venus (Ref. 4), suggest a value of 6050 ± 0.5 km for the radius of Venus. In addition, *Mariner V* ranging data combined with simultaneous radar data² give a radius of 6056.6 ± 2.1 km. The radar radius of 6048 km measured at Arecibo (Ref. 4) was selected as the gravitational potential surface defining the upper bound surface pressure for the models. It is doubtful that the entire discrepancy in radius can be attributed to topography. Asymmetry in the shape of the planet is estimated to be on the order of only 1 km.

Thus, the resolution of an appropriate uncertainty range for the mean Venus surface pressure is a direct consequence of the uncertainty in the location of the planetary mean surface radius. The surface pressure, as interpreted from the *Venera 4* data (16.4 to 20.3 atm), could be as high as 167 atm if the radar radius is correct and the *Venera 4* probe did not, in fact, impact at the instant of final data transmission. Although arguments have been made that the Soviet probe did indeed transmit data up to the time of surface impact (Ref. 5), the case in favor of the radar surface seems the most plausible. Thus, the data are bimodal in nature, the planetary surface and atmospheric parameters being related to the radius defined by superimposing the *Mariner V* and *Venera 4* data in one case, and to the radar radius in the other. The likelihood of the planetary radius being somewhere in between appears remote. Consequently, the specification of a mean model would appear unjustified.

References

1. McElroy, M. B., "The Upper Atmosphere of Venus," *J. Geophys. Res.*, Vol. 73, No. 5, Mar. 1, 1968.
2. Kliore, A., et al., "Atmosphere and Ionosphere of Venus from the *Mariner V* S-Band Radio Occultation Measurement," *Science*, Vol. 160, Dec. 29, 1967.
3. Avduevskiy, V. S., Marov, M. Ya., and Rozhdestvenskiy, M. K., "The Model of the Atmosphere of the Planet Venus on the Results of Measurements Made by the Soviet Automatic Interplanetary Station *Venera 4*," *J. Atmos. Sci.*, Vol. 35, No. 4, July, 1968.
4. Ash, M., et al., "The Case for the Radar Radius of Venus," *Science*, Vol. 160, May 31, 1968.
5. Reese, D., and Swan, P., "*Venera 4* Probes the Atmosphere of Venus," *Science*, Vol. 159, Mar. 15, 1968.

²Anderson, J. D., et al., "The Radius of Venus As Determined By Planetary Radar and *Mariner V* Radio Tracking Data," paper presented at the American Astronomical Society meeting, Victoria, British Columbia, Aug. 20-23, 1968.

B. Application of Thermal Modeling to Space Vehicle Sterilization, A. R. Hoffman and J. T. Wang

1. Introduction

Planetary quarantine constraints may necessitate the application of a dry-heat thermal sterilization process to a planetary capsule prior to launch. To minimize the severity of the sterilization cycle and also to assure the desired level of sterility, it is necessary to account for the reductions in microbial population that occur during the transient phases of heating and cooling, as well as the reductions that occur during the steady-state phase. Geometric and analytic capsule models have been developed and applied to (1) provide insight into the relationships existing between the characteristics of the microbial populations and the thermal characteristics of the space vehicle and heating medium, and (2) perform sensitivity studies prior to subjecting the hardware to a sterilization environment.

2. Geometric Analytic Model

Numeric analytic techniques used to establish sterilization processes in the food and pharmaceutical industries were adapted to provide a first approximation of the calculation necessary for the development of capsule dry-heat sterilization process parameters. A simplified geometric conceptual model of a space vehicle was constructed. The space vehicle was assumed to be a series of cylindrical shells (see SPS 37-47, Vol. III, Fig. 1, p. 32) made of homogeneous material with insulated ends. Each shell was mated to the other in such a manner that the heat flow through the model was as through an infinite cylinder. The dimensions of the model were arbitrary but were chosen to approximate the dimensions of a large planetary landing vehicle. The model is not representative of any space vehicle configuration but was developed to facilitate the transition of the numeric analytic techniques from food containers to space vehicles.

Using the geometric model, some important conclusions were drawn (SPS 37-47, Vol. III, pp. 31-35, and Refs. 1 and 2):

- (1) Verification that consideration of the microbial reduction that occurs during the transient phases of the sterilization cycle can result in a significant reduction in total process time.
- (2) Indication that the distribution of microbial load upon the space vehicle may significantly affect the calculations of the required process parameters and therefore is necessary information for proper process calculation.

- (3) Indication that, as the effective thermal conductivity increases, the required sterilization process time will decrease.
- (4) Demonstration that the process calculations are sensitive to changes in certain microbial heat resistance parameters (D values³) and relatively insensitive to other heat resistance parameters (z values³).

3. Capsule Analytic Model

To apply the numeric analytic concept to hardware, the feasibility capsule of a possible Mars entry and landing vehicle (Fig. 5) was analytically modeled as illustrated in Fig. 6. The capsule analytic model was divided

³Term D is the decimal reduction time, or time at temperature required to destroy 90% of the microorganisms. Term z is numerically equal to the number of degrees Fahrenheit (or centigrade) required for a thermal destruction curve to traverse one logarithm cycle.

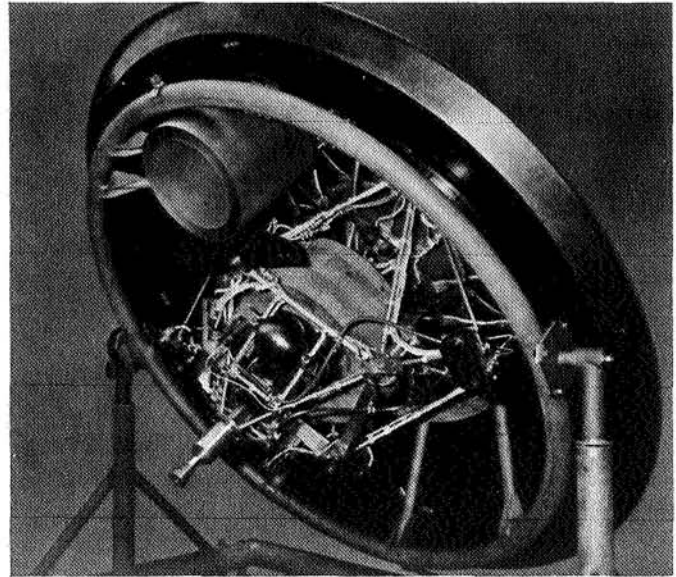


Fig. 5. Feasibility model—separation configuration

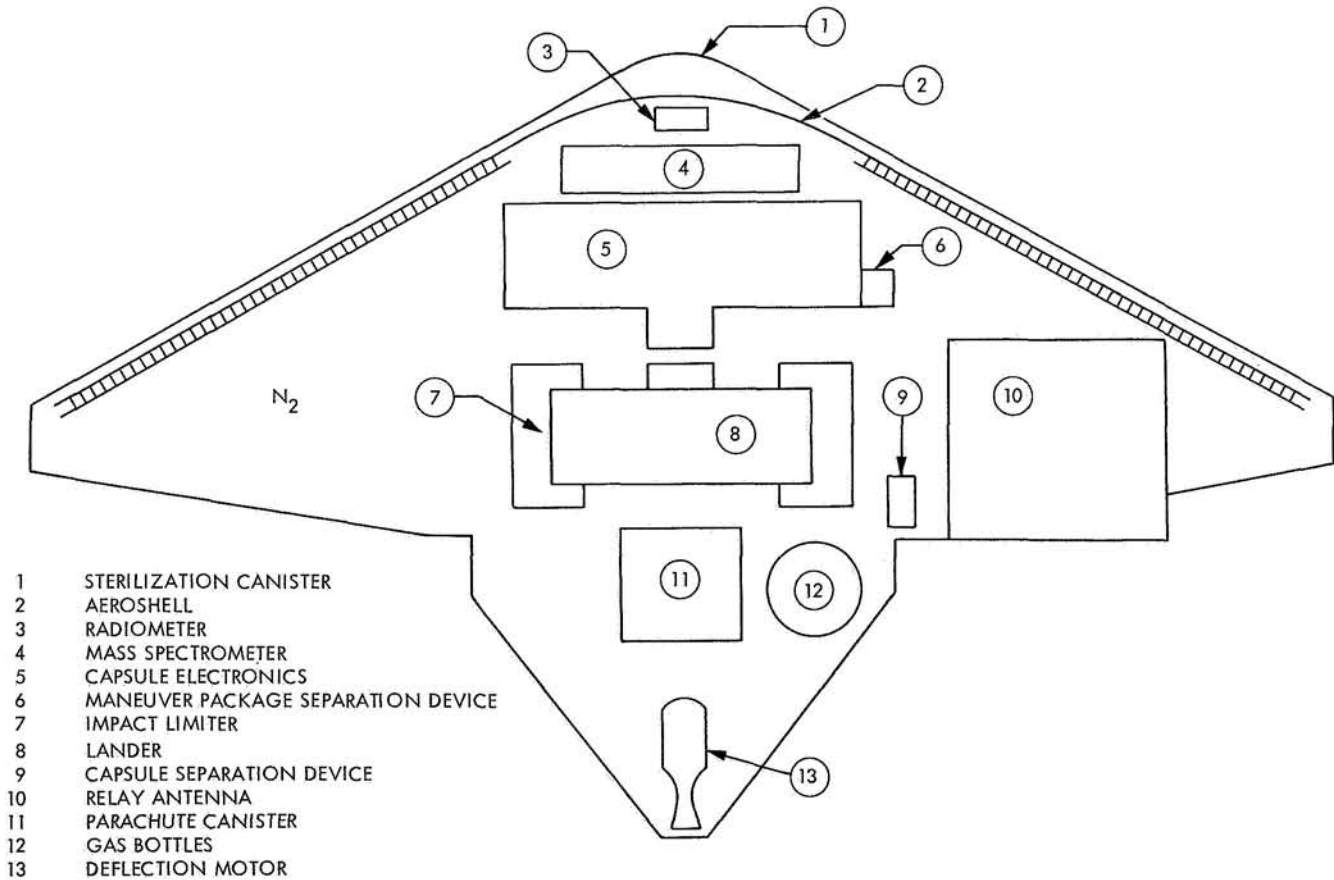


Fig. 6. CSAD thermal model

into 72 thermal nodes with 4 gaseous nitrogen nodes located within the canister; the canister itself was divided into 6 nodes to provide the capability of accounting for nonuniformity of temperatures. In order to provide length-of-cycle alternatives during the sterilization process, the thermal analysis bracketed a wide range of possible temperature responses and a wide range of possible microbial burden numbers that could exist after the cycle had begun. The predictions for a family of heating profiles used in determining the length-of-cycle alternatives are shown in Fig. 7. These curves were used for the sterilization of the capsule system advanced development (CSAD) flight model (Ref. 3).

An attempt was also made to optimize the sterilization cycle for the capsule by analyzing the effects of variations in heating and cooling rates on total process times. The

boundary conditions for the heating and cooling rate evaluation included the following cases:

- (1) A driving temperature rate R_c of $11^\circ\text{C}/\text{h}$ was applied to the sterilization canister. The interior portions of the capsule were heated and cooled by natural convection and conduction through the nitrogen gas atmosphere inside the canister. Then, higher heating rates R_c of 19, 25, and $40^\circ\text{C}/\text{h}$ were individually applied to the canister. [A rate of $40^\circ\text{C}/\text{h}$ was believed to be the maximum capability of the terminal sterilization chamber (TSC).]
- (2) A hot gas with a heating and cooling rate R_g of $11^\circ\text{C}/\text{h}$ was forced through the capsule (while in the TSC with R_c of $11^\circ\text{C}/\text{h}$) with a flow rate of $40\text{ ft}^3/\text{min}$ through an 8-in. port.

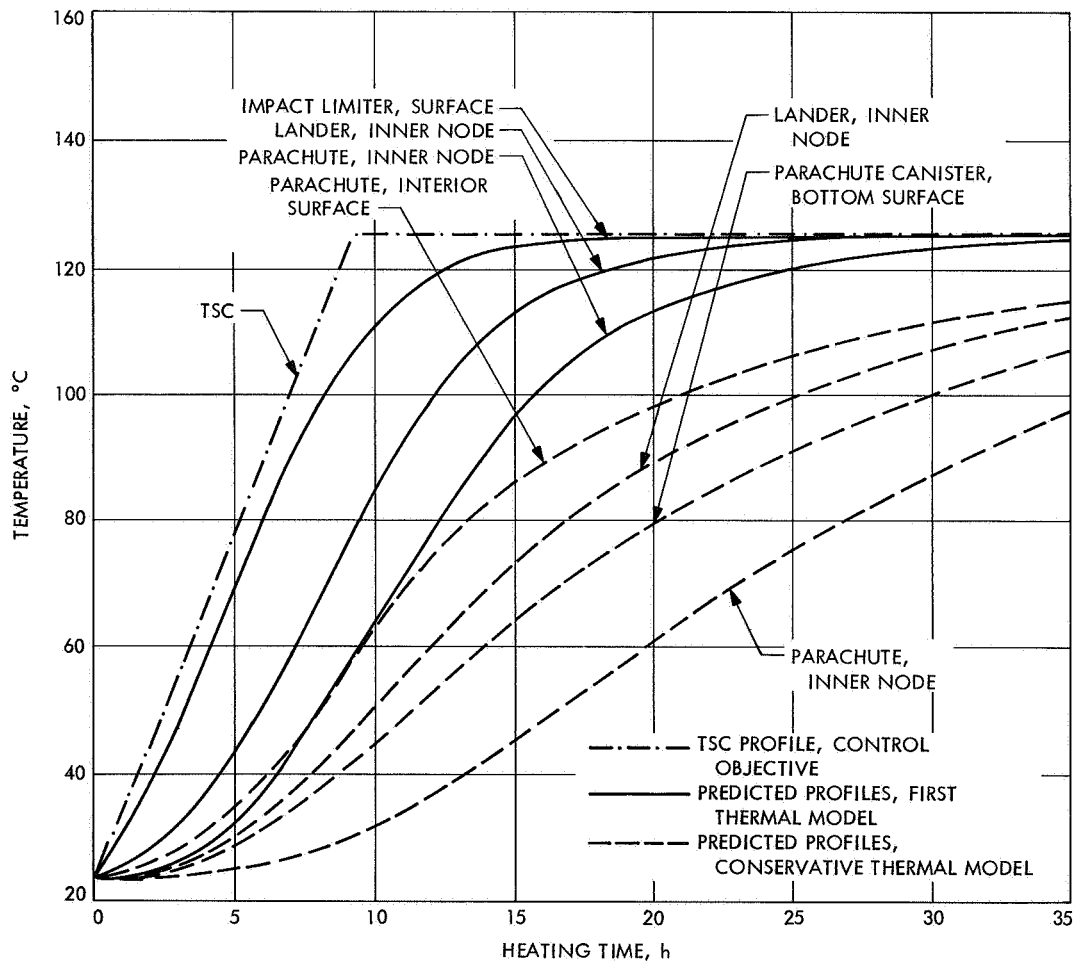


Fig. 7. CSAD heating profiles—system sterilization

4. Results

Important results of this analysis to the particular capsule configuration considered included:

- (1) As R_c increased, the heat application time decreased, but the time needed to be at 125°C increased (Table 3).⁴ This is attributed to the larger lethality occurring during the transient phases for the cycles with slow heating and cooling rates. If the time a subsystem is at 125°C can be used as a measure of severity, a subsystem with low-thermal mass, such as the radiometer, would experience a more severe sterilization environment at the 40°C/h rates than at the 11°C/h rate even though the same sterility level is achieved.
- (2) There was no significant reduction noted in heat application time between the case where the cap-

⁴Lethality calculation assumptions: initial number of microorganisms $N_0 = 10^4$, probability of survival $P_s = 10^{-4}$, $z = 25^\circ\text{C}$, lethality begins at 100°C.

sule was "baked" in a gas environment and the case where the gas was forced through the canister.

Further applications using thermal models are being performed to better define and understand the parametric relationships existing in space vehicle sterilization processes.

References

1. Hoffman, A. R., and Stern, J. A., *Terminal Sterilization Process Calculation for Spacecraft*, Technical Report 32-1209. Jet Propulsion Laboratory, Pasadena, Calif., Nov. 15, 1967. (Also appears in *Developments in Industrial Microbiology*, Vol. IX, pp. 49-64, 1968.)
2. Stern, J. A., and Hoffman, A. R., *Determination of Terminal Sterilization Process Parameters*, Technical Report 32-1191. Jet Propulsion Laboratory, Pasadena, Calif., Oct. 1, 1967. (Also appears in *Proceedings of COSPAR*, London, July 1967.)
3. Hoffman, A. R., "Determination of the Terminal Sterilization Cycle for a Possible Mars Capsule," *Proceedings of the AAS-AIAA Rocky Mountain Symposium*, Denver, Colo., July 1968.

Table 3. CSAD process times for different heating and cooling rates

Parameter	Analysis case 1				Analysis case 2, gas following 11°C/h	Assumed D_{125} value
	11°C/h	19°C/h	25°C/h	40°C/h		
Aeroshell surface						
Maximum temperature, °C	118	118	119	118	120	20 min
Heat application, h	13.5	11.2	10.7	9.0	11.6	
TSC at 125°C, h	4.1	5.8	6.6	6.4	2.2 ^a	
Total process, ^b h	32.0	27.2	26.9 ^c	25.4	25.6	
Parachute canister surface						
Maximum temperature, °C	117	118	117	117	118	20 min
Heat application, h	14.7	12.8	12.0	11.0	13.7	
TSC at 125°C, h	5.3	7.4	7.9	8.4	4.3 ^a	
Total process, ^b h	36.0	32.7	31.0 ^c	29.5	32.3	
Lander inner node						
Maximum temperature, °C	122	122	122	122	122	40 min
Heat application, h	20.0	18.0	17.5	17.0	19.2	
TSC at 125°C, h	10.6	12.6	13.4	14.4	9.8 ^a	
Total process, ^b h	40.9	36.5	35.8 ^c	35.1	37.5	

^aTime canister atmosphere at 125°C.

^bSum of heat application (time from 23°C to maximum temperature) and cooling (time from maximum temperature to 25°C).

^cEstimated, cooling profile not complete.